

IMPROVEMENT OF OZONE DETECTION WITH WO₃ ORIENTED FILMS

Julien OLLITRAULT¹, Nicolas MARTIN^{1*}, Jean-Yves RAUCH¹, Jean-Baptiste SANCHEZ², Franck BERGER²

¹Institut FEMTO-ST, UMR 6174, Université de Franche-Comté, CNRS, ENSMM, UTBM, 15B, Avenue des
montboucons, 25030 Besançon Cedex, France

²Laboratoire de Chrono-Environnement, UMR 6249, Université de Franche-Comté, CNRS, UFR ST La Bouloie, 16,
Route de Gray, 25030 Besançon Cedex, France

Abstract

Tungsten oxide WO₃ thin films were prepared by dc reactive magnetron sputtering. The GLancing Angle Deposition (GLAD) technique was implemented to transform the typical dense microstructure into an inclined columnar and porous architecture. The incident angle α of the sputtered particles was 0 and 70° leading to a column tilt angle β of 0 and 40°, respectively. Conventional and inclined WO₃ films were sputter deposited on a commercial hotplate system. Ozone gas was periodically injected from 0 to 220 ppb and the variation of resistance of the system was measured vs. time at 250°C. The conventional WO₃ films exhibited a significant change of conductance as a function of the ozone injection. GLAD WO₃ films with a columnar angle $\beta = 40^\circ$ were even more sensitive to the ozone pulses and the time of response or recovery was significantly enhanced. This ozone detection improvement was mainly attributed to the more porous structure of WO₃ films produced by the GLAD method.

Keywords: GLancing Angle Deposition; WO₃ thin films, porosity, ozone detection.

1. Introduction

Enhancement of the gas detection requires the development of novel materials and thin films in which the surface interactions with gaseous species have to be investigated. Small size, easy use and flexibility in fabrication are the main advantages of chemoresistive-type semiconductor sensors based on metal oxide compounds. Among such compounds, tungsten trioxide (WO₃) appears as an interesting material for the gas detection since it is an indirect

* Corresponding author: nicolas.martin@femto-st.fr; Tel.: +33 (0)3 63 08 24 31; Fax: +33 03 81 66 67 01

28 band gap n-type semiconductor sensitive to very low concentrations of toxic gases like Cl_2 , SO_2 , CH_4 or O_3 [1-3].
29 When gases interacts with tungsten trioxide, surface conductivity changes take place mainly due to variations of the
30 free electron concentration occurring by charge exchange with adsorbed species. It is commonly admitted that the
31 sensitivity of the metal oxide to ozone is mainly due to the presence of surface oxygen vacancies [4]. Several doping
32 strategies were developed in order to favor this type of vacancies and improve the gas sensor performances [5-8].
33 Another approach consists in tuning the structure of thin films in order to produce porous architectures at the micro
34 and nanoscales [9, 10]. To this aim, the GLAD method (GLancing Angle Deposition) is an elegant way for growing
35 films exhibiting original and porous structures (inclined columns, zigzags, helices ...) using physical vapor
36 deposition processes such as magnetron sputtering [11].
37 In this letter, we show that sensors utilizing WO_3 thin films sputter deposited by GLAD strongly improve the
38 detection of ozone. A classical WO_3 film produced with a normal incidence of the particle flux is compared to an
39 inclined columnar WO_3 GLAD film. Both materials are similarly tested as gas sensors in an ozone environment.
40 Response and recovery times, repeatability and sensitivity of these systems are compared taking into account the
41 difference of architectures produced by conventional and GLAD sputtering.

42

43 **2. Material and methods**

44 Films were deposited by reactive dc magnetron sputtering. A stainless-steel home made vacuum reactor (volume of
45 40 L) was equipped with a circular planar and water cooled magnetron sputtering source. It was evacuated with a
46 turbomolecular pump, backed by a mechanical pump, in order to reach an ultimate pressure of 10^{-5} Pa. A tungsten
47 target (purity 99.9 at. %, 51 mm diameter) was dc sputtered using a constant current $I = 50$ mA. The pumping speed
48 was set constant at $S = 13$ L s^{-1} . Argon flow rate was kept at 2.4 sccm and oxygen flow rate was maintained at 2
49 sccm, corresponding to argon and oxygen partial pressures of 3×10^{-1} and 3×10^{-2} Pa, respectively. Substrates,
50 introduced through a 1 L airlock, were glass microscope slides and (100) silicon wafers (p-type, $\rho = 1-30$ Ωcm).
51 Before each run, all substrates were cleaned with acetone and alcohol, and the target was pre-sputtered in a pure
52 argon atmosphere for five minutes before injecting oxygen, in order to remove the target surface contamination
53 layer. Afterwards, oxygen gas was introduced and the process was stabilized for 10 minutes. The target to substrate
54 distance was kept at 50 mm in all runs. Substrates were grounded and all depositions were carried out at room
55 temperature. The deposition time was adjusted in order to obtain a thickness close to 1 μm . Morphological features

56 of the samples were probed by scanning electron microscopy (SEM) at 15 keV. Films produced on (100) Si were
57 used to observe architecture and cross-section morphology. WO₃ thin films were sputter deposited on a commercial
58 MSP769 Heraeus sensor. Such a device allows a simultaneous heating, temperature and resistance measurements vs.
59 time during the gas test. The later was performed at 250°C (optimized temperature not shown) according to a
60 procedure further described in [12]. O₃ was periodically supplied by means of UV irradiation of a dry air flow (200
61 mLmin⁻¹ at 0.2 % of relative humidity) combined with a dilution bench leading to an accurate injection of 220 ppb
62 following a rectangular signal. The conductance change of the coated device was measured as a function of time.

63

64 **3. Results and discussion**

65 Films deposited with a conventional incident angle ($\alpha = 0^\circ$) exhibit a poorly defined cross-section morphology (Fig.
66 1a). A dense packed structure can be distinguished with major fracture directions, which are perpendicular to the
67 film/substrate interface. This kind of feature is typical of amorphous oxides prepared by reactive sputtering at room
68 temperature. Some better defined columns are clearly observed for WO₃ films produced with an incident angle $\alpha =$
69 70° (Fig. 1b). An inclined columnar architecture is achieved with narrow columns (a few tens of nanometers) and a
70 column angle $\beta = 40^\circ$. As usually reported with the GLAD process, this column angle β is systematically lower than
71 the incident angle α [13]. It is dependent upon many factors including the type of sputtered materials, growth
72 temperature, composition, energy of particles, shadowing effect, etc. Several analytical equations have been
73 proposed in the literature providing different predictive relationships between α and β [14]. They systematically lead
74 to the conclusion that the column inclination angle (β) always lies between the film normal and the vapor incidence
75 angle and strongly varies with the deposition conditions. It is worth noting that the SEM cross-section of GLAD
76 WO₃ films also displays a more voided structure. As shadowing is enhanced for larger incident angles ($\alpha > 70^\circ$ is
77 considered as the beginning of extreme shadowing regime), it results in formation of more isolated columns and thus
78 a more porous material. The relationship between α and film density can be made via geometric analysis of oblique
79 deposition [15]. Density models and experimental measurements all show a significant drop of the film density as α
80 reaches 60° . For our WO₃ films prepared with $\alpha = 70^\circ$ and taking into account a simple geometric approach from
81 Tait *et al.* [16], one can assume a normalized film density of 51 %. It means that nearly half part of the GLAD films

82 is occupied by void regions, which correlates with the important intercolumnar spacing previously noticed from the
83 SEM cross-section observations (Fig. 1b).

84 The dynamic sensing transients of the conventional ($\alpha = 0^\circ$ and $\beta = 0^\circ$) and GLAD ($\alpha = 70^\circ$ and $\beta = 40^\circ$) WO_3 thin
85 film sensors towards pulses of 220 ppb of O_3 at 250°C are reported in Fig. 2. Ozone was periodically injected using
86 a constant flow for 1200 s and stopped for 1800 s. The normalized sensor conductance $\Delta G/G_{air}$ vs. time t was plotted
87 setting G_{air} as the conductance in dry air and $\Delta G = G_{air} - G_{oz}$ where G_{oz} is the conductance in the presence of ozone.
88 Since WO_3 is an n-type semiconductor and ozone is an oxidizing gas, the conductance of the both type of sensors (β
89 $= 0$ and 40°) decreases when exposed to ozone (reduction mechanism of O_3 molecules). For both WO_3 films, a drift
90 of the $\Delta G/G_{air}$ signal can be noticed as the number of ozone injections increases. It tends to become negligible after
91 a few periodic injections, which means that the sensors tend to be stable. For conventional WO_3 sensor ($\beta = 0^\circ$),
92 $\Delta G/G_{air}$ drops from 1 down to 0.12 at the end of ozone exposure (after 1200 s). By stopping the ozone injection,
93 $\Delta G/G_{air}$ rapidly restores to 1 before the next pulse. A cyclic gas injection correlates with periodic and repeatable
94 responses of the sensor following exponential signals, which are typical of performant systems exhibiting adsorption
95 and desorption mechanisms vs. time.

96 Sensors coated with the WO_3 GLAD film ($\alpha = 70^\circ$ and $\beta = 40^\circ$) also show a clear response when ozone is
97 periodically supplied (Fig. 2). Exponential growth and decay of the normalized variation of conductance as a function
98 of time is similarly measured. It is worth noticing the more pronounced and rapid evolution of the sensor signal as
99 ozone is injected or stopped. Following the same pulsing procedure as previously implemented for conventional
100 samples, $\Delta G/G_{air}$ is lower than 0.06 at the end of the first ozone injection and tends to be null after a couple of
101 cycles. This extended variation of the signal corresponds to enhanced sensitivity of the WO_3 GLAD sensor. In
102 addition, the time required to reach a nearly stable conductance ratio is also improved as especially recorded on the
103 third ozone pulse. Last but not least, response time as well as recovery time are both boosted. They can be
104 quantitatively estimated from the slope of the curve when ozone is injected and stopped, respectively. Taking into
105 account the beginning of the ozone injection, $|\partial(\Delta G/G_{air})/\partial t| = 2.5 \times 10^{-3} \text{ s}^{-1}$ for WO_3 films with $\beta = 0^\circ$ whereas it is
106 more than $3.6 \times 10^{-3} \text{ s}^{-1}$ for $\beta = 40^\circ$. On the other hand, when ozone is stopped, the return to the background signal is
107 also more defined for WO_3 GLAD film since $\partial(\Delta G/G_{air})/\partial t = 5.0 \times 10^{-3} \text{ s}^{-1}$ whereas it reaches only $2.3 \times 10^{-3} \text{ s}^{-1}$ for
108 conventional WO_3 film. It is commonly admitted that performances of sensors based-on WO_3 compounds (or other

109 oxides) are directly connected to the atomic defects in the films, especially oxygen deficiencies. Zhang *et al.* [17]
110 have reported that WO_{3-y} films exhibit a metallic appearance for $y > 0.5$ and become transparent for $y < 0.3$. In our
111 films, both samples (conventional with $\alpha = 0^\circ$ and GLAD with $\alpha = 70^\circ$) are transparent and the oxygen flow rate
112 used during the deposition is high enough to deposit stoichiometric WO_3 compound. So, the improvement of the
113 ozone detection cannot be only assigned to oxygen deficiencies but has to be correlated with the architecture, i.e.
114 strongly dependent on the voided structure favored by the GLAD process. In addition, it was previously shown that
115 GLAD films become strongly porous for $\alpha > 60^\circ$ (due to extreme shadowing). Oxidation of the film is also
116 enhanced when heated at 250°C [18]. Thus oxygen deficiencies are strongly reduced and cannot be considered as
117 the main criterion influencing the sensor performances. Inclined columnar structure is also kept in spite of the
118 temperature rising as previously shown for similar compounds [19] or for more reactive systems based on titanium
119 oxide [20]. As a result, we can claim that stoichiometric GLAD WO_3 films are produced and the improvement of the
120 ozone detection is mainly attributed to the increase of the specific surface in GLAD films. Our results are in
121 agreement with a few investigations focused on the detection of NO_2 , water vapor or other gaseous species
122 implementing WO_3 GLAD thin films [9, 10, 19]. This enhanced response of the GLAD sensors was mainly assigned
123 to the porous nanostructure with high surface-to-volume ratio (more than several order of magnitudes higher specific
124 area than dense planar film). In addition to high sensitivity, long-term reliability, short response and recovery times
125 and based-on changes of conductance reported in figure 2, one can expect that the detection limit reached by such
126 nanostructured WO_3 films should be below the sub-ppb level [10].

127

128 **4. Conclusions**

129 Ozone sensors were fabricated by coating commercial Heraeus devices with WO_3 thin films. Reactive dc magnetron
130 sputtering was implemented to deposit these tungsten oxide films. A conventional process was used to prepare dense
131 and poorly structured thin films whereas the GLancing Angle Deposition method (GLAD) was developed to
132 produce oriented and well defined columnar architectures. The GLAD WO_3 films were produced by means of an
133 incident angle of the particle flux $\alpha = 70^\circ$ leading to a column tilt angle $\beta = 40^\circ$. The conductance response of the
134 sensors maintained at 250°C was measured vs. time when they were submitted to a pulsed and periodic injection of
135 ozone. It was shown that both type of films were sensitive to this gas. However the WO_3 GLAD films exhibited a
136 stronger effect on the shape of the response curve. These oriented films showed superior ozone sensing

137 performances especially highest and fastest responses and recovery times towards ozone at an operating temperature
138 of 250°C. This enhanced sensing characteristics were mainly attributed to the large surface area favored by the
139 GLAD process. A more porous and voided structure was produced by GLAD giving rise to more active surface
140 sites. The open and porous microstructure emphasized by this approach makes these films ideal candidates for
141 sensing applications. Gaseous species can readily interact with the high-surface area peculiar to the inclined
142 columnar architectures. Future experiments require dilution tests and other inclinations of the columnar structure.
143 Other architectures will also be explored in next works.

144

145 **Acknowledgements**

146 This work was supported by the Region of Franche-Comté (FIMICAP and MATECO projects) and performed in
147 cooperation with the Labex ACTION program (contract ANR-11-LABX-01-01).

148

149 **References**

- 150 [1] G.F. Fin, L.M. Cavanagh, A. Afonja, R. Binions, *Sensors*, 10 (2010) 5469-5502.
- 151 [2] K. Wetchakun, T. Samerjai, N. Tamaekong, C. Liewhiran, C. Siriwong, V. Kruefu, A. Wisitsoraat, A.
152 Tuantranont, S. Phanichphant, *Sens. Actuators B*, 160 (2011) 580-591.
- 153 [3] S.M. Kanan, O.M. El-Kadri, I.A. Abu-Yousef, M.C. Kanan, *Sensors*, 9 (2009) 8158-8196.
- 154 [4] S.R. Utembe, G.M. Hansford, M.G. Sanderson, R.A. Freshwater, K.F.E. Pratt, D.E. Williams, R.A. Cox, R.L.
155 Jones, *Sens. Actuators B*, 114 (2006) 507-512.
- 156 [5] E. Rossignol, A. Prim, E. Pellicer, J. Arbiol, F. Hernandez-Ramirez, F. Peiro, A. Cornet, J.R. Morante, L.A.
157 Solovyov, B. Tian, T. Bo, D. Zhao, *Adv. Funct. Mater.*, 17 (2007) 1801-1806.
- 158 [6] B.T. Marquis, J.F. Vetelino, *Sens. Actuators B*, 77 (2001) 100-110.
- 159 [7] A. Hoel, L.F. Reyes, P. Heszler, V. Lantto, C.G. Granqvist, *Current Applied Physics*, 4 (2004) 547-553.
- 160 [8] S. Zhu, X. Liu, Z. Chen, C. Liu, C. Feng, J. Gu, Q. Liu, D. Zhang, *J. Mater. Chem.*, 20 (2010) 9126-9132.
- 161 [9] J.J. Steele, M.T. Taschuk, M.J. Brett, *Sens. Actuators B*, 140 (2009) 610-615.
- 162 [10] H.G. Moon, Y.S. Shim, D.H. Kim, H.Y. Jeong, M. Jeong, J.Y. Jung, S.M. Han, J.K. Kim, J.S. Kim, H.H. Park,
163 J.H. Lee, H.L. Tuller, S.J. Yoon, H.W. Jang, *Scientific Reports*, 2(588) (2012) 1-7.

- 164 [11] M.W. Hawkeye, M.T. Taschuk, M.J. Brett, "Glancing Angle Deposition of Thin Films", John Wiley & Sons,
165 Ltd, Chichester, 2014.
- 166 [12] A. Gaddari, F. Berger, M. Amjoud, J.B. Sanchez, M. Lahcini, B. Rhouta, D. Mezzane, C. Mavon, E. Beche, V.
167 Flaud, Sens. Actuators B, 176 (2013) 811-817.
- 168 [13] K. Robbie, J.C. Sit, M.J. Brett, J. Vac. Sci. technol., B16(3) (1998) 1115-1122.
- 169 [14] R. Alvarez, L. Gonzalez-Garcia, P. Romero-Gomez, V. Rico, J. Cotrino, A.R. Gonzalez-Elipe, A. Palmero, J.
170 Phys. D: Appl. Phys., 44 (2011) 385302-7.
- 171 [15] C. Buzea, K. Robbie, J. Optoelectron. Adv. Mater., 6(4) (2004) 1089-1097.
- 172 [16] R.N. Tait, T. Smy, M.J. Brett, Thin Solid Films, 226 (1993) 196-201.
- 173 [17] J.G. Zhang, D.K. Benson, C.E. Tracy, S.K. Deb, A.W. Czanderna, C. Bechinger, J. Electrochem. Soc., 144
174 (1997) 2022-2026.
- 175 [18] A. Besnard, N. Martin, F. Sthal, L. Carpentier, J.Y. Rauch, Funct. Mater. Lett., 6(1) (2013) 1210051-5.
- 176 [19] M. Horprathum, K. Limwichean, A. Wisitsoraat, P. Eiamchai, K. Aiempnanakit, P. Limnonthakul, N.
177 Nuntawong, V. Pattantsetakul, A. Tuantranont, P. Chindaudom, Sens. Actuators B, 176 (2013) 685-691.
- 178 [20] N. Martin, J. Sauget, T. Nyberg, Mater. Lett., 105 (2013) 20-23.

179

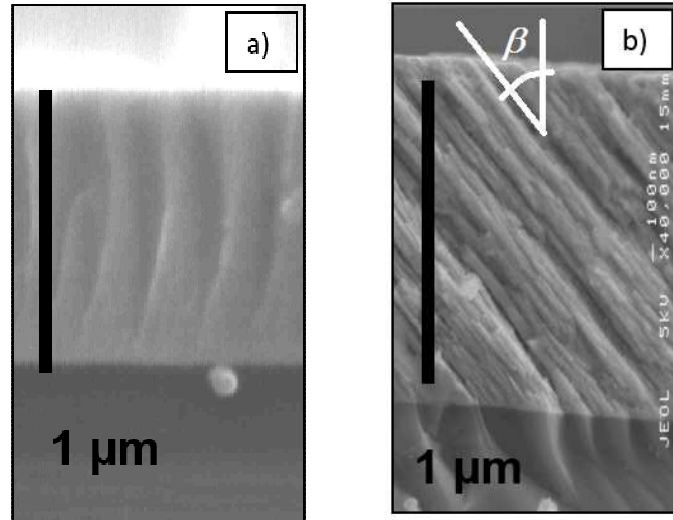
180 **Figure captions**

181 **Fig. 1.** SEM cross-section micrographs of WO₃ thin films prepared a) with a normal incidence ($\alpha = 0^\circ$ and $\beta = 0^\circ$);
182 b) by GLAD ($\alpha = 70^\circ$ and $\beta = 40^\circ$)

183 **Fig. 2.** Ozone injection profile and corresponding normalized conductance $\Delta G/G_{air}$ vs. time t of WO₃ thin films with
184 normal incidence ($\alpha = 0^\circ$ and $\beta = 0^\circ$) and by GLAD ($\alpha = 70^\circ$ and $\beta = 40^\circ$).

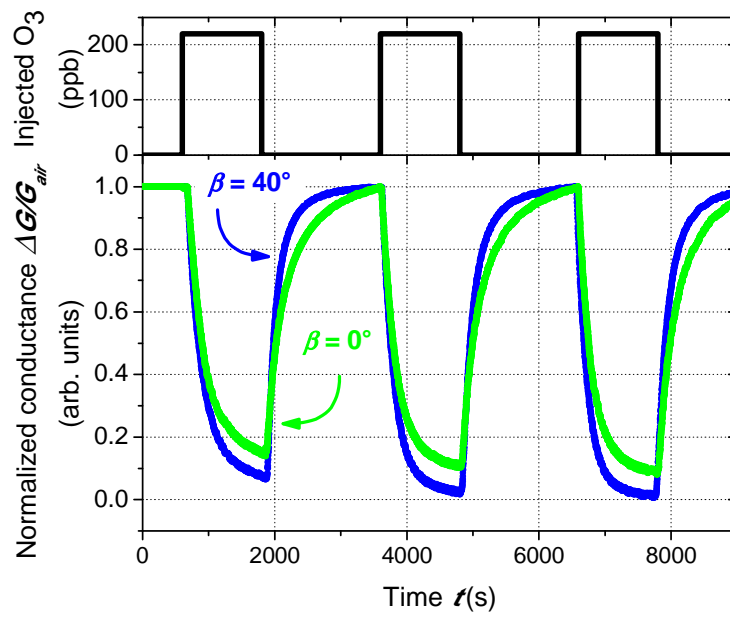
185

186 **Figure 1**



187

188 **Figure 2**



189